NASA Technical Memorandum 89897

The Impact Damped Harmonic Oscillator in Free Decay

G.V. Brown
Lewis Research Center
Cleveland, Ohio

and

C.M. North
Rose-Hulman Institute of Technology
Terre Haute, Indiana

Prepared for the
Vibrations Conference
sponsored by the American Society of Mechanical Engineers
Boston, Massachusetts, September 27–30, 1987

NASA

THE IMPACT DAMPED HARMONIC OSCILLATOR IN FREE DECAY

G.V. Brown
National Aeronautics and Space Administration
Lewis Research Center
Cleveland, Ohio 44135

and

C.M. North
Rose-Hulman Institute of Technology
Terre Haute, Indiana 47803

ABSTRACT

The impact-damped oscillator in free decay is studied by using time history solutions. A large range of oscillator amplitude is covered. The amount of damping is correlated with the behavior of the impacting mass. There are three behavior regimes: (1) a low amplitude range with less than one impact per cycle and very low damping, (2) a useful middle amplitude range with a finite number of impacts per cycle, and (3) a high amplitude range with an infinite number of impacts per cycle and progressively decreasing damping. For light damping the impact damping in the middle range is (1) proportional to impactor mass, (2) additive to proportional damping, (3) a unique function of vibration amplitude, (4) proportional to $1-\epsilon$, where ϵ is the coefficient of restitution, and (5) very roughly inversely proportional to amplitude. The system exhibits jump phenomena and period doublings. An impactor with 2 percent of the oscillator's mass can produce a loss factor near 0.1.

NOMENCLATURE

A	nondimensional oscillator amplitude
a	coefficient of sine term in oscillator displacement
b	coefficient of cosine term in oscillator displacement
c	proportional damping constant
d	total gap between impactor and cavity walls
k	oscillator spring constant
m	oscillator mass
T	average nondimensional oscillator period with impactor present ($= 2\pi\sqrt{1+\mu}$)
T_i	period for approximately repetitive motion of impactor
t	time
t_i	time of impact
t_o	time of zero crossing of oscillator displacement
x	oscillator displacement
$\dot{x}$	oscillator velocity
$\ddot{x}$	oscillator acceleration
x_o	initial oscillator displacement for a time interval between impacts
$\dot{x}_o$	initial oscillator velocity for a time interval between impacts
$\dot{x}_-$	oscillator velocity immediately before an impact
$\dot{x}_+$	oscillator velocity immediately after an impact
y	displacement of impactor relative to oscillator
$\dot{y}$	velocity of impactor relative to oscillator
$\dot{y}_-$	impactor relative velocity immediately before impact
$\dot{y}_+$	impactor relative velocity immediately after impact
ϵ	coefficient of restitution
ζ	viscous damping ratio of oscillator
η	loss factor ($(2\pi)^{-1}$ times fraction of energy lost to damping per cycle)
η_i	loss factor due to impact damping only
μ	impactor mass ratio (impactor mass divided by oscillator mass)

φ_i phase of an impact, measured in degrees from most recent zero crossing of oscillator

ω_n undamped natural frequency of oscillator

ω_o damped natural frequency of oscillator

INTRODUCTION

The impact damper has been studied for several decades (Popplewell, et al. (1983), Masri (1970), Bapat and Sankar (1985), and references therein) because it produces substantial damping for its mass and because it is effective over a wide frequency range. There is extensive literature on the related topics of impacts in systems with mechanical clearance such as pinned joints, gear trains, cams, and pistons (see for example Bapat, et al. (1983) and references therein). The impact-damped system is a linear system only between impacts, and closed form solutions of its motion are not obtainable. Before the advent of large computers, most of the progress in predicting the forced response of the damper was made by searching for steady-state solutions with special characteristics and by examining the stability of the solutions. These methods have been supplemented by analogue and digital time-history solutions. The focus of the time-history solutions has tended to remain on steady-state forced response and on limited ranges of oscillator amplitude.

The present study is motivated by a desire to add damping to very lightly damped aerospace systems that undergo forced or self-excited vibration (flutter). The inherent loss factor (fraction of vibrational energy dissipated per radian) is often less than 0.01 and sometimes below 0.001. Small additions to damping in these systems could greatly increase component life or, by relieving design constraints imposed to avoid excessive vibration, could permit performance gains or weight savings.

Besides providing damping predictions for these systems, the focus on light damping in free decay reveals features of impact damper behavior that are not observable in more heavily damped systems because any given range of amplitude is traversed more rapidly. In this study the mass of the impacting particle (impactor) is at most 4 percent of the oscillator mass, and the loss factor is usually less than 0.1. Extremely light impactors (0.001 percent of the primary mass) are used to explore limiting behavior.

The study of free decay is perhaps not, in itself, as important as the study of forced response, and a thorough response study should be made before applying impact dampers in aerospace systems. However, a free decay study has value in this nonlinear problem for several reasons. First, there are features of the behavior of the impactor in free decay which carry over into forced behavior but which are less easily recognized there because of the complexity and diversity of behavior. Secondly, a single transient decay can elicit a range of impact behavior from below one to an infinite number of bounces per cycle and an amplitude range covering over two orders of magnitude. On the other hand, behavior in narrow ranges of amplitude can be studied in detail by using very light impactors. Finally the results have intrinsic value in showing the rate of recovery from a transient disturbance.

DECAY CALCULATIONS

A simple harmonic oscillator damped by an impactor in a cavity is represented in figure 1. The equations of motion and their solutions, presented in the appendix, are simple in any interval between successive impacts. The impacts are modeled by assuming that a coefficient of restitution exists, and the equations that relate the velocities before and after impacts appear in the appendix. The equations are made dimensionless by using the cavity gap d as the length unit, the primary mass m as the mass unit, and the reciprocal (in sec/radian) of the undamped natural frequency ω_n of the harmonic oscillator as the time unit. A FORTRAN computer code was written to calculate time histories of the motion and several other functions of time (described in the appendix). The system is completely specified by the mass fraction μ of the impactor, the coefficient of restitution ε, the proportional damping ratio ζ of the oscillator (stemming from viscous, material or structural damping) and the initial conditions of motion. Proportional damping was included to see how it interacts with impact damping in the nonlinear system. The influence of initial conditions on the results was not explored; the oscillator was released without velocity from its initial amplitude.

Decay curves of the nondimensional amplitude A of the oscillator for $\varepsilon = 0.6$ are shown in figure 2. Values of μ are 1, 2, and 4 percent, and there is 0.01 percent of critical viscous damping in the oscillator system. The slopes of the curves show that the impact damping increases as the amplitude decreases, except near the low-amplitude end of each curve. Also shown for the $\mu = 1$ percent curve are keys to figures 3 and 4, which present short segments of the impactor motion to show representative impact patterns that occur at various amplitudes. In figure 3 the impactor displacement is shown relative to its cavity walls, located at relative displacements of the impactor of 0 and 1. In figure 4 absolute displacements of the impactor and of the walls are shown. Note the variety of impact patterns. These include (some not shown in the figures) equal numbers of impacts on each side (figs. 3(b), 4(a) and 4(b)), an even number on one side and an odd number on the other (fig. 3(c)), and patterns that repeat only after two or more cycles. At oscillator amplitudes above ~5 the number of impacts on each side of the cavity becomes infinite, as for a ball bouncing to rest, but the time elapsed during such a "bounce-down" is finite. A typical case is shown in figure 3(a). Slower decay occurs below an amplitude of about 0.05 because the impactor lacks enough speed to traverse the cavity in less than one cycle, as shown in figure 4(c). This range will be called the range of impact failure.

The reason for high damping for amplitude on the order of a few tenths of the cavity gap can be seen in figure 4(b). At the amplitude illustrated there, the impactor travels several times as far as the oscillator, hence it has a higher velocity. It acquires this velocity through impacts on an advancing wall. At the amplitude where maximum damping occurs, the impactor velocity is approximately five times the maximum velocity of the oscillator. In the restitution model, a fraction of the relative velocity is lost at each impact. Thus the high relative velocity due to impacts

on an advancing wall is responsible for the high damping.

Previous authors have noted the wide variety of impact behavior in this and related systems in both analytical and experimental studies of forced response (Masri (1970), Valuswami, et al (1975), Popplewell et al. (1983), Bapat, et al. (1983), and Bapat and Senkar (1985)). The present study provides a unifying limiting case for a number of previous studies because inside an oscillator undergoing free decay under sufficiently light damping, the motion of the oscillator is essentially unperturbed. Hence in the light damping limit the distinction between the harmonic oscillator and a housing driven in sinusoidal motion vanishes. Similarly the distinction between forced response and of free decay through the same amplitude range vanishes. Thus two important connections can be made between the present results and published work on impactors in driven housings (Bapat, et al. (1983)) and in forced harmonic oscillators with light damping (Masri (1970), and Popplewell, et al. (1983)).

There remain some questions of how closely the impactor behavior in free decay corresponds to that in forced response or in the driven housing. It is known that two impact patterns can be stable under the same conditions in a driven housing (Bapat, et al. (1983)). Yet the behavior of the impactor in an oscillator in free decay is uniquely determined by the initial conditions, and hence only a single behavior (i.e. impact pattern) is possible during the pass through any given amplitude. (However, other initial conditions may yield a different behavior at the given amplitude.) On the other hand in a freely decaying oscillator, the impactor passes through complex and possibly even chaotic states which may not exist in a steady state and which stability theory could not predict. For example in the transitions between regular impact patterns during oscillator decay, a very light impactor passes through a large array of impact patterns that approximate the "long-period" (and possibly chaotic) behavior found possible by previous authors studying impact systems (see for example, Shaw (1985). Thus one-to-one correspondence of impactor behavior in a decaying oscillator with that in a forced oscillator or in a driven housing is not expected. In spite of these unexplored questions of correspondence between free decay, forced response, and driven housings, a considerable degree of correspondence in impactor behavior is shown, and the loss factor calculations for free decay have value for feasibility studies.

LOSS FACTOR RESULTS

Figure 2 presented decay curves of the oscillator amplitude for three values of μ. The loss factors, computed from those decays by using the amplitudes in five successive cycles to smooth fluctuations (see the appendix), are presented in figure 5 as functions of the amplitude. As expected from the slopes of the curves in figure 2, the loss factor increases as the amplitude decreases, until amplitude is between 0.05 and 0.1. In this range impact failure occurs and the damping drops abruptly toward the proportional damping value. Erratic bounces still occur, sometimes causing a temporary increase in the oscillator energy and amplitude. The averaging process used in calculating the loss factor reduces the height and broadens the damping peaks in figure 5 because very low values from the impact failure range are mixed in. This effect is greater for larger μ.

Note the considerable similarity of the curves in figure 5. Dividing the loss factor by μ reduces the curves very nearly to a single curve, as shown in figure 6. (Aside from the peak region affected by averaging, the main visible differences occur at the highest amplitude (lowest damping) and arise from the proportional damping. These can be removed as shown below.) Thus for μ up to 4 percent, the impact loss factor per unit mass fraction of the impactor, henceforth called the specific loss factor, is a constant at any given amplitude. This is to be expected for very light damping where the impactor barely perturbs the oscillator motion. The energy dissipated in an impact and hence the loss factor are then proportional to the impactor mass. A portion of the specific loss factor curve for $\mu = 0.25$ percent is included as a dashed line to show the approximate shape that the peak of the curves would have without averaging. (For the lighter impactor, the slower decay yields more oscillator cycles in any amplitude range. The effects of averaging are thus more localized.)

Figure 7 presents the loss factor curves for a single mass fraction, 2 percent, but for various values of proportional damping ζ. Curves for proportional damping ratios ζ between 0.01 and 0.8 percent are shown. To find out whether the total damping is a simple sum of impact and proportional damping, the loss factor corresponding to the proportional damping was subtracted from each curve. (Note that loss factor η and viscous damping ratio ζ are related by $\eta = 2\zeta$.) The results, divided by the impactor mass fraction to yield specific impactor loss factor, are plotted in figure 8. The curves are almost identical, justifying the ordinate label of specific "impactor loss factor," and showing that the proportional damping in the main oscillator and the impact damping are additive in the light damping regime. Thus a single universal function of amplitude describes the specific impactor loss factor. This universality applies only to various values of mass fraction and of proportional damping, however; a change of the coefficient of restitution produces a new function, as is shown later.

Over a substantial portion of the universal impactor damping curve (fig. 8) the impactor damping appears to vary roughly inversely with amplitude. To show to what extent this is true, the specific impactor loss factor multiplied by the amplitude is plotted in figure 9. Over the amplitude range between 0.1 and 10, the curves lie within ±30 percent of 0.34. That is,

$$A\eta_i/\mu = 0.34\ (1\pm0.3) \qquad (0.1 < A < 10,\ \epsilon = 0.6)$$

where η_i is the loss factor due to the impactor. This equation provides an estimate of impact damping over a wide amplitude range. Note that the bounce-down range is made more visible in this type of plot. It is the range of predominantly negative slopes above the maxima near $A = 5$.

The approximate constancy of $A\eta_i/\mu$ leads to a characteristic of the impact damped oscillator noted in previous experimental and analytical studies, namely the near-linear decay of amplitude with time (see, e.g., Bapat and Sankar (1985)). Since the loss factor η_i is proportional to the amplitude decay rate

divided by A, then if A_{n_j} is roughly constant, the decay rate must be roughly constant.

Results presented up to this point have been for $\epsilon = 0.6$, a value within the range for steel-on-steel impacts (0.5 to 0.8), (Higdon and Stiles (1955)). To show the general effect of changing ϵ, the impactor loss factor is presented in figure 10 for three values of ϵ, 0.4, 0.6, and 0.8. It is seen that reducing ϵ raises the impact damping in the middle range of amplitude. But bounce-down ends at lower amplitudes for lower ϵ, and the amplitude below which impact failure occurs rises as ϵ falls. It appears that A_{n_j}/μ may be linear with $\ln(A)$ and independent of ϵ in the bounce-down range. As ϵ increases the damping curve becomes more erratic in most ranges of amplitude. It also appears from figure 10 that within the active range of the impactor the damping is roughly proportional to $(1 - \epsilon)$. This is shown to be the case in figure 11 where the ordinate variable is $A_{n_j}/(\mu(1 - \epsilon))$. Unfortunately the fluctuations in the $\epsilon = 0.8$ curve are magnified by a factor of 5 by dividing by $(1 - \epsilon)$.

IMPACT PHASE, PERIOD DOUBLING, POSSIBLE CHAOS, AND JUMP PHENOMENA

The impact pattern of the impactor in a freely decaying oscillator becomes more definite and has richer detail if the total damping (viscous plus impact) is reduced to allow slower passage through each amplitude. A number of interesting features of such a slow decay can be brought out by plotting the time of each impact during a half cycle as a function of the oscillator amplitude. Remnants of many features can then be identified in similar plots for faster decays. In these plots it is convenient to use the oscillator phase angle (measured in degrees from the oscillator zero crossing) as the measure of time, as described in the appendix.

Figure 12 presents a plot of impact phases for $\mu = 0.001$ percent. This extremely light impactor barely perturbs the oscillator. (The value of ζ was chosen to yield the desired record length.) The very slow decay encompasses about 1900 oscillator periods and nearly 8000 impacts. Each impact is represented by an open circle in the figure, but where the impactor motion becomes repetitive, the circles merge into smooth bold lines. With reference to plots like those in figures 3 and 4, one can identify the impact patterns that occur in each amplitude range. A single impact at the same phase in each half cycle occurs for $A < 0.35$. Similarly two impacts per half cycle, repeated every half cycle, occur for $1.2 < A < 1.4$; three for $2.4 < A < 2.6$; and four for $3.4 < A < 3.55$. At the high amplitude end of each of these regions (i.e., at $A = 0.35$, 1.4, 2.6, and 3.55), each phase line splits into two branches. The number of impacts per oscillator cycle does not change at these points, but rather the impacts occur at different phases in successive half cycles. The density of impact points along each branch is thus half of that on the coalesced curve. To the left of the splits, the smallest "period" T_j for repetitive behavior of the impact phase is 180°, or half of the oscillator period T. To the right of the splits the impact phase period T_j is 360° and is thus equal to T. Most of the split phase lines can be followed to another split at a higher amplitude (e.g., at $A = 1.57$, 2.73, and 3.65), where T_j becomes 720° or $2T$. And by expanding the scales, at least one additional phase "period doubling" can be seen in some cases. Period doubling is known to be one route to chaos (bounded, nonperiodic motion). This raises the question (beyond the scope of this study) of whether there is a chaotic region between every adjacent pair of orderly impact regimes. Chaos does occur in an impactor mounted with a spring and proportional damping in a driven housing (Shaw (1985).

In a nonlinear system where more than one state of motion exists for a given set of parameters, jumps between the states can occur as some parameter is slowly changed. Here jumps between states of differing impact periodicity can occur with amplitude changes. Such jumps can be seen by comparing an impact phase graph for free decay with one taken from a calculation in which the amplitude is made to grow with time by specifying a negative value of the viscous damping ratio for the primary oscillator. (Negative values of viscous damping can be used to describe self-excited oscillations such as flutter.) Two phase graphs so obtained are shown in figures 13(a) and (b). In both figures $\mu = 0.001$ percent and $|\zeta| = 0.02$ percent, but ζ is negative in (b). Note the tendency of the impactor in each case to maintain trends of its impact pattern. For example during growth the condition of two equally spaced impacts per cycle (denoted by 2e) persists to $A = 0.4$, whereas in decay that pattern sets in only below 0.36.

The regions of regular impactor behavior in figure 13 can be compared with the regions of stable impactor behavior inside a housing driven at various steady sinusoidal amplitudes presented in Bapat et al. (1983). Stable impact regimes for $\epsilon = 0.6$ from that paper are shown in figures 13(a) and (b) denoted by asterisks. The boundaries of the 2e region in decay are very close to those of Bapat et al. (1983). The phases of the impacts in the 2e region agree very well with those predicted from the analysis in that paper. In the region of two unequally spaced impacts per cycle (denoted by 2u for the present calculations and by 2u* for data from Bapat et al. (1983)), the phase from that paper, figure 4 agrees with the phase of the earlier of the two impacts of the present results below about $A = 0.4$, but there the Bapat et al. (1983) phase turns upward. The regions of three impacts per oscillator period (labeled as above), show greater differences. For example in both growth (fig. 13(b)) and decay (fig. 13(a)) there are regions marked 8,3 in which there are eight impacts in three cycles (with two impacts in the first cycle, three in the second and three in the third). Other more irregular impact patterns are present in $0.79 < A < 0.88$, but three impacts per oscillator period are the most common. Clearly during growth and decay, periodic behavior is only approximated, and various impact patterns occur in transitions that may not be stable in a steady state.

Figure 13(a) also shows some period doublings. At $A = 0.35$ two unequally spaced impacts per cycle become two equally spaced impacts, hence the impact period above $A = 0.35$ is twice that below. In the region above $A = 0.48$, where three impacts per cycle predominate, the range $0.48 < A < 0.53$ has an impact phase period equal to the oscillator period T. From $A = 0.53$ to 0.64 the impact phase period is $2T$. A small region around $A = 0.65$ has an impact phase period of $4T$.

At higher values of impactor mass fraction, the grosser features of the impact phase graphs are maintained, but detail is lost because fewer impacts occur per unit range of amplitude. With faster decay the

identifiable features shift toward lower amplitude. Figure 14 shows impact phase for $\mu = 0.02$ and $\zeta = 0.0001$ over the amplitude range up to 10. Doublings of impact phase period are still visible for 1 through 6 impacts per half cycle. The doubling at $A = 1.4$ in figure 12 has shifted to near $A = 1.3$. The range where bounce-down occurs ($A > 5$) is included in figure 14, and in that range an additional phase point is plotted when the impactor is thrown free at a phase near 180°. This region has received little attention in the literature on impact dampers. It was discussed as a special case under the term translated as "slippage" in Fedosenko and Feigin (1971) and references therein. It is not a favorable regime for impact damping; the impactor loss factor is two orders of magnitude lower than at the peak near $A = 0.1$.

CONCLUDING REMARKS

The damping produced by a relatively light impactor (~1 to 4 percent of the oscillator mass) is substantial in comparison to the levels inherently present in many turbomachinery components. Whereas the inherent loss factors for blades often lie between 0.001 and 0.01, even a 2 percent impactor mass fraction can yield an impact loss factor of 0.1 at the most effective amplitude and above 0.01 over a wide amplitude range. Thus the possibility of significant flutter suppression and of order-of-magnitude reductions in resonant vibration exists for applications where impactors can be designed to work near their optimum amplitude range. The small mass required may permit the use of combinations of impactors with different gaps to afford high damping over wide ranges of amplitudes.

Some aspects of forced response of impact damped systems (e.g., small amplifications of motion when the oscillator is driven at a frequency below its natural frequency) are not illuminated by these free decay results. But near resonance, where most vibration problems are of practical importance, the free decay results have reasonable predictive value. Furthermore, the free decay results directly show the rate of recovery from excitation by a short transient disturbance.

Frequency tuning, which limits the effectiveness of the tuned vibration absorber to the vicinity of the resonance for which it is designed, is not present in the impact damper. However, it is replaced by what might be called amplitude tuning; the effectiveness of impact damping is a very strong function of amplitude, being highest when the amplitude is about 10 percent of the impactor gap for $\epsilon = 0.6$, falling off abruptly at lower amplitudes and falling roughly inversely with amplitude at higher amplitudes.

The origin of the highest damping, obtained when one impact occurs in each half cycle, was shown to lie in the high velocity of the impactor caused by the occurrence of the impacts when the oscillator is advancing toward the impactor.

Several factors permit approximate prediction of impact damping in the light damping regime. Impact damping is (1) directly additive to the proportional damping of the oscillator, (2) proportional to the impactor mass, (3) roughly proportional to $(1 - \epsilon)$ in the "active" regime for the impactor, and (4) (for a very rough approximation) approximately inversely proportional to amplitude.

The dependence of impact damping upon amplitude was shown to be correlated with the impact pattern. The graphs of impact phase as a function of amplitude illuminated the impact patterns in considerable detail and showed examples of period doubling, evidence of possible chaotic behavior and the existence of jump phenomena.

REFERENCES

Bapat, C.N., Popplewell, N., and McLachlan, K. 1983, "Stable Periodic Motions of an Impact-Pair," Journal of Sound and Vibration, Vol. 87, No. 1, pp. 19-40.

Bapat, C.N., and Sankar, S., 1985, "Single Unit Impact Damper in Free and Forced Vibration," Journal of Sound and Vibration, Vol. 99, No. 1, pp. 85-94.

Fedosenko, Iu. S., and Feigin, M.I., 1971, "Periodic Motions of a Vibrating Striker Including a Slippage Region," PMM: Journal of Applied Mathematics and Mechanics, Vol. 35, No. 5, pp. 844-850.

Higdon, A., and Stiles, W.B., 1955, Engineering Mechanics, Second ed., Prentice-Hall, New York, p. 509.

Masri, S.F., 1970, "General Motion of Impact Dampers," Journal of the Acoustical Society of America, Vol. 47, No. 1, Pt. 2, pp. 229-237.

Popplewell, N., Bapat, C.N., and McLachlan, K., 1983, "Stable Periodic Vibroimpacts of an Oscillator," Journal of Sound and Vibration, Vol. 87, No. 1, pp. 41-59.

Shaw, S.W., 1985, "The Dynamics of a Harmonically Excited System Having Rigid Amplitude Constraints, Part I: Subharmonic Motions and Local Bifurcation, Part II: Chaotic Motions and Global Bifurcations, Journal of Applied Mechanics, Vol. 52, No. 2, pp. 453-464.

Sollar, P.J., 1985 "The Development of a Computer Model as an Aid to the Solution of the Problem of Impact Damping," MA Thesis, Rose-Hulman Institute of Technology, Terra Haute, IN.

Veluswami, M.A., Crossley, F.R.E., and Horvay, G., 1975, "Multiple Impacts of a Ball Between Two Plates, Part II: Mathematical Modelling," Journal of Engineering for Industry, Vol. 97, No. 3, pp. 828-835.

APPENDIX - DERIVATION OF EQUATIONS

Between two successive impacts the equations of motion are simply those of a damped harmonic oscillator and of a free particle. Well separated bounces are treated by assuming that a coefficient of restitution exists. A separate procedure is used for a "bounce down," as discussed below. When the particle is at rest on a wall the equation of motion is that of a damped harmonic oscillator with increased mass. A second special situation occurs when the stuck impactor is thrown free of the main oscillator.

Motion Between Well-Separated Impacts

The equation of motion of the oscillator with mass m, spring constant k and proportional damping constant c is

$$\ddot{x} + 2\zeta\omega_n\dot{x} + \omega_n^2 x = 0 \qquad (1)$$

where $\omega_n = \sqrt{k/m}$ is the undamped natural frequency and $\zeta = c/(2m\omega_n)$ is the viscous damping ratio. One form of the solution is

$$x = (a \sin \omega_o t + b \cos \omega_o t)e^{-\zeta\omega_n t} \qquad (2)$$

where we take time t equal to zero at the most recent impact, and $\omega_o = \omega_n \sqrt{1 - \zeta^2}$ is the damped natural

frequency. If the oscillator displacement and velocity immediately after that impact are x_0 and $\dot{x}_0$, then the constants a and b are given by

$$b = x_0$$
$$a = (\dot{x}_0 + x_0\zeta\omega_n)/\omega_0 \tag{3}$$

Between impacts the impactor has a constant velocity.

Equations for Well-Separated Impacts

In the restitution model

$$\dot{y}_+ = -\epsilon\,\dot{y}_- \tag{4}$$

If the velocities of the oscillator before and after an impact are $\dot{x}_-$ and $\dot{x}_+$, then conservation of total momentum requires

$$\dot{x}_+ + \mu(\dot{x}_+ + \dot{y}_+) = \dot{x}_- + \mu(\dot{x}_- + \dot{y}_-) \tag{5}$$

By using (4) to eliminate $\dot{y}_+$ from (5), we obtain

$$\dot{x}_+ = \dot{x}_- + \mu(1 + \epsilon)\dot{y}_-/(1 + \mu) \tag{6}$$

The value of $\dot{y}_+$ from (4) is the initial impactor relative velocity for the new time interval. The value of $\dot{x}_+$ from equation (6) becomes the initial velocity $\dot{x}_0$ of the oscillator during the new interval and is used to determine the new value of the constant a in equation (3). The positions of the two masses are unchanged by the impact, because the impact is assumed to occur in an infinitesimal increment of time.

The time of impact is obtained by calculating the relative displacement of the impactor at regular small time intervals until impact occurs. Then the impact time is found to the desired accuracy by the method of bisection.

Impactor Bouncing to Rest Relative to the Oscillator

The impactor can come to relative rest on either wall of the cavity in a finite time with an infinite number of bounces. This happens at high oscillator amplitudes A ($A \geq 5$ for $\epsilon = 0.6$ and $\mu \leq 8$ percent). The solution of the equations interval-by-interval described above must be abandoned during bounce-down because of the infinite number of time intervals. The finite time to come to relative "rest" can be estimated if the acceleration $\ddot{x}$ of the oscillator is fairly constant during the bounce-down process. Infinite sums giving the total time to come to rest and the remaining impulse transferred to the oscillator can be evaluated in closed form. However, this is not accurate when the bounce-down approaches an oscillator phase near 180°, which occurs during free decay just before the system leaves the bounce-down regime (near $A = 5$ in fig. 14). The present results do not utilize the infinite sums. Instead the impacts were followed until the time between them was deemed suitably short and then the next bounce was assumed to occur with zero restitution, initiating a "stuck" condition. A similar method of treating bounce-down is presented by Soller (1985) with details of nondimensionalizing the equations of motion and their solutions. After bounce-down is complete, the two masses move as one as long as the impactor is stuck.

Stuck Impactor

The equation of motion and its solution for the combined system of the oscillator and the impactor are of the same forms as for the oscillator alone. Several of the constants must be changed to reflect the increase in mass by the factor $(1 + \mu)$.

Sling-Free of Stuck Impactor

The stuck impactor remains on a cavity wall as long as the oscillator acceleration is toward the impactor. When the acceleration changes sign, the impactor is thrown free. In the absence of damping and forcing in the oscillator system, this would occur at the equilibrium position of the oscillator, but with either present the exact time of the acceleration sign change must be found. This time was found in the same way as for impact times.

Use of Dimensionless Variables

To facilitate computations and to obtain results in a general form, the equations were put in nondimensional form. The cavity gap d is the unit of length. The mass m of the oscillator is the mass unit and in terms of it the impactor mass is the mass fraction μ. The time unit is ω_n^{-1}, the reciprocal of the undamped natural frequency. The undamped period of oscillation is 2π in the absence of the impactor, and the damped period is negligibly different for the small values of ζ used herein. With an impactor present the period is slightly irregular when the impact pattern does not repeat in successive cycles, but its average value is $2\pi\sqrt{(1 + \mu)}$, except in the impact failure range.

Calculation of Loss Factor and Impact Phase

The loss factor is defined as the fraction of vibrational energy dissipated per radian. It is also twice the fraction of amplitude decrease per radian in a free decay. (Note that for $\mu = 0$, one radian is one unit of nondimensional time, but for $\mu > 0$, one radian of actual motion spans $\sqrt{1 + \mu}$ nondimensional time units. The amplitude was calculated every half cycle. A least squares parabolic fit of the amplitudes in five successive cycles was used to determine the decay rate and the loss factor. This smoothing procedure was used because some impact patterns cause considerable fluctuations of amplitude.

The phase of the impacts during a half cycle was measured from the time t_0 of the most recent zero crossing of the oscillator displacement. The phase φ_i of any impact, measured in degrees was calculated from

$$\varphi_i = 180^\circ\,(t_i - t_0)/(\pi\sqrt{1 + \mu}) \tag{7}$$

where t_i and t_0 are nondimensional times. The use of (7) gives the phase compared to an average period.

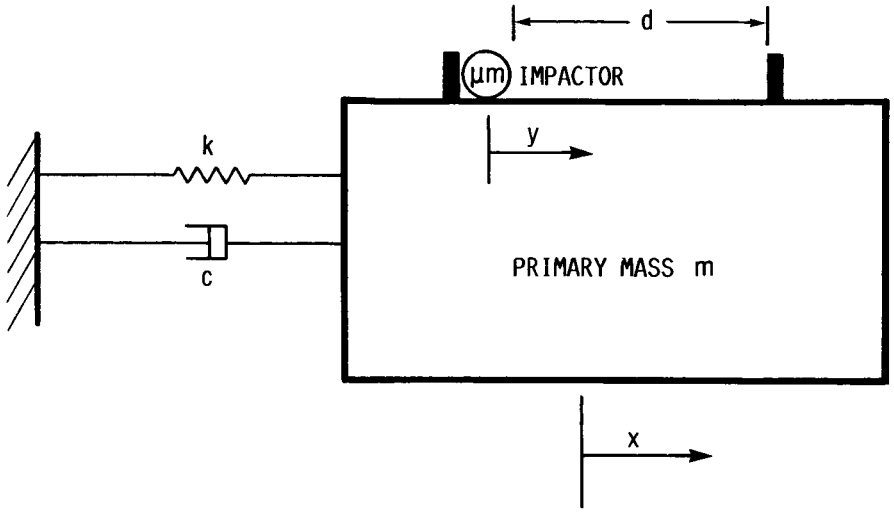

FIGURE 1. - SCHEMATIC OF IMPACT-DAMPED HARMONIC OSCILLATOR.

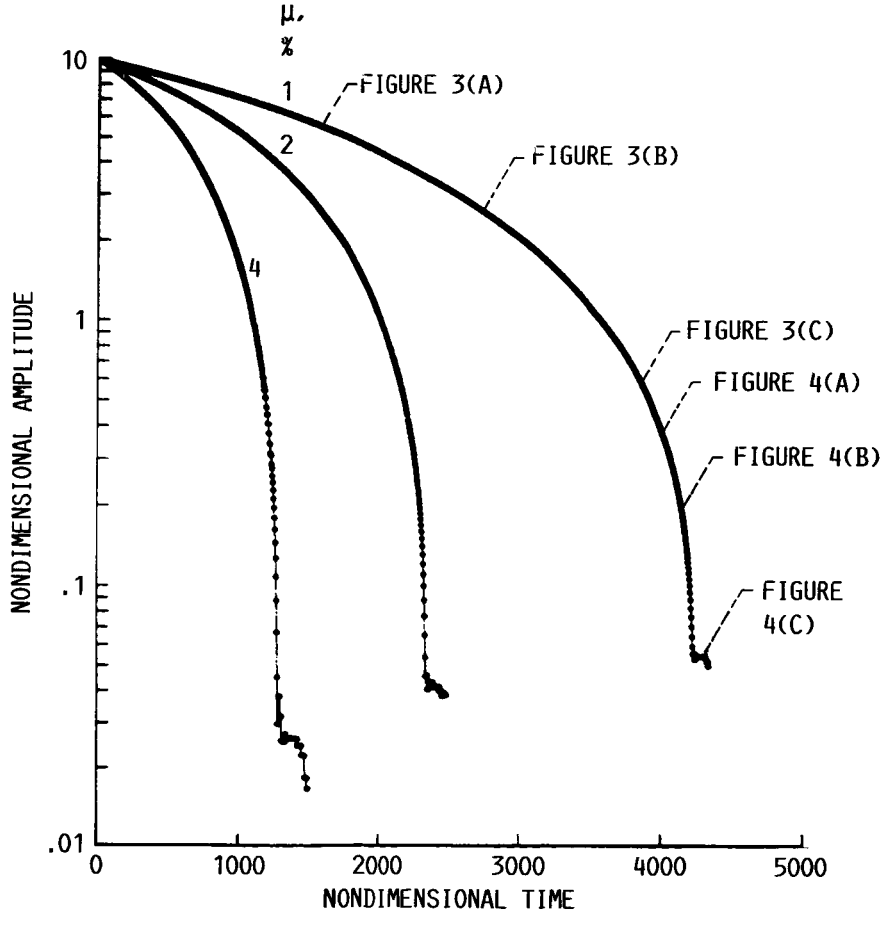

FIGURE 2. - AMPLITUDE DECAY CURVES WITH KEYS TO IMPACT PATTERNS IN FIGURES 3 AND 4; $\zeta = 0.0001$; $\varepsilon = 0.6$.

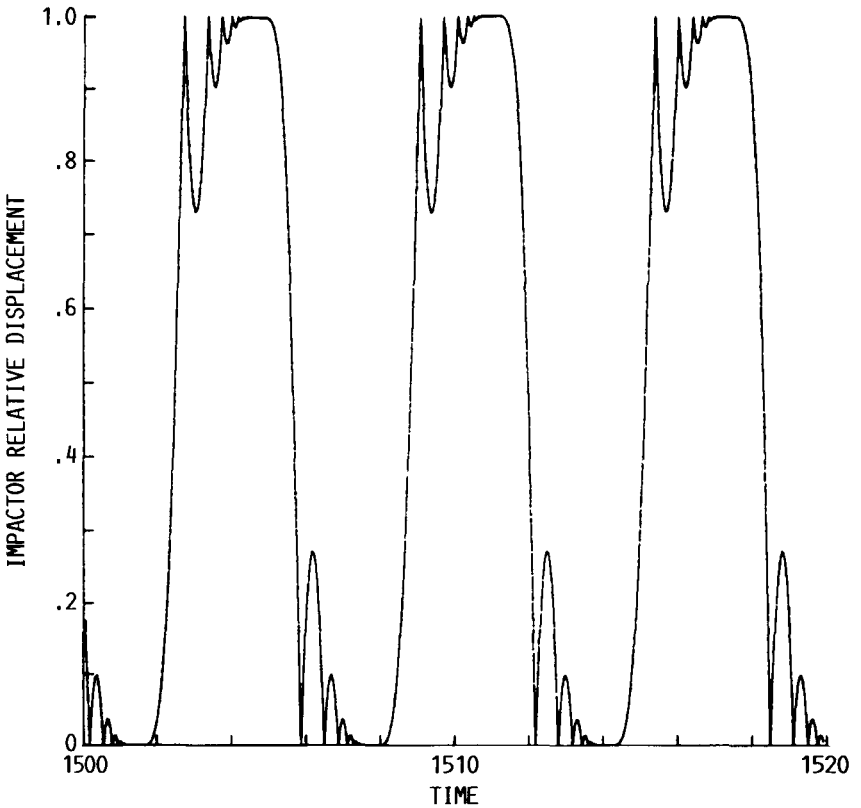

(A) AMPLITUDE, ~5.6; INFINITE NUMBER OF IMPACTS EACH HALF CYCLE.

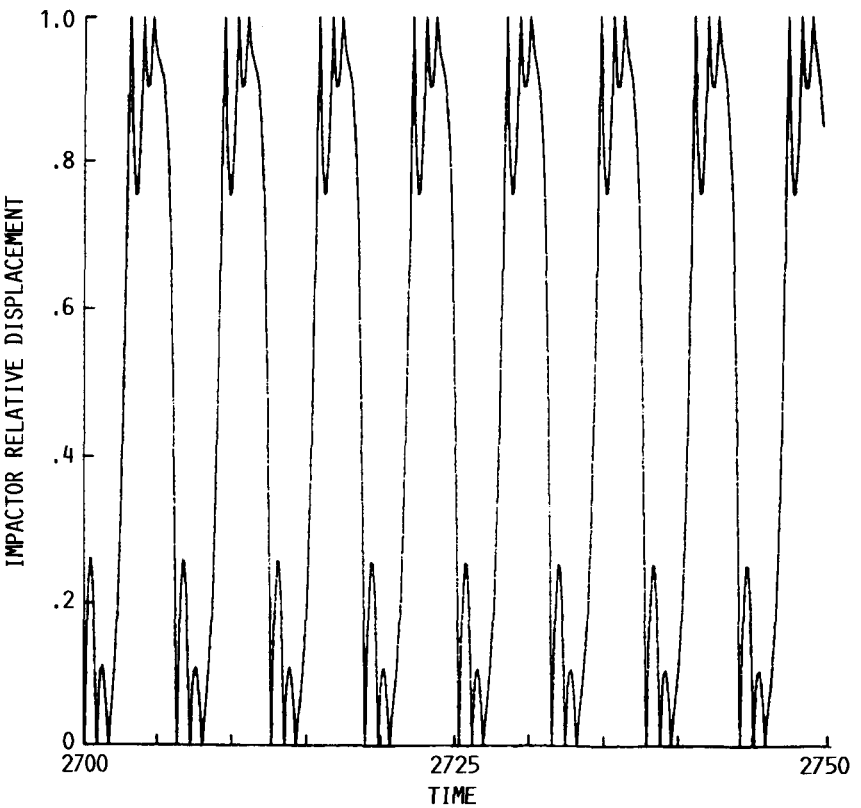

(B) AMPLITUDE, ~2.6; THREE IMPACTS EACH HALF CYCLE.

FIGURE 3. - IMPACTOR DISPLACEMENT SHOWN RELATIVE TO CAVITY WALLS.

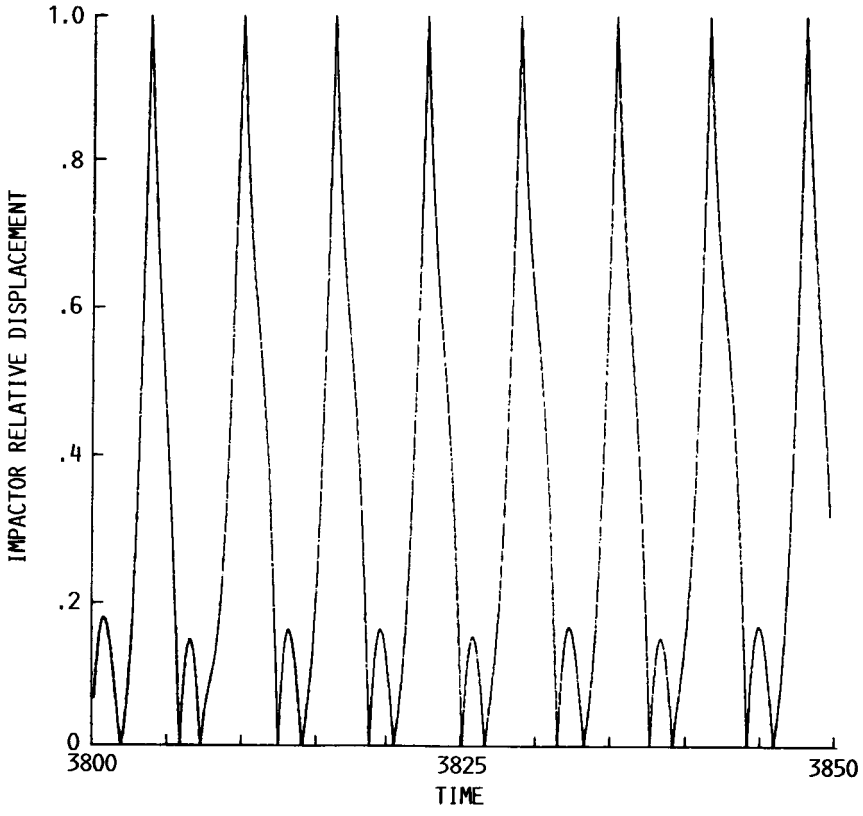

(C) AMPLITUDE, ~0.6; ONE IMPACT PER HALF CYCLE ALTERNATING WITH TWO.

FIGURE 3. - CONCLUDED.

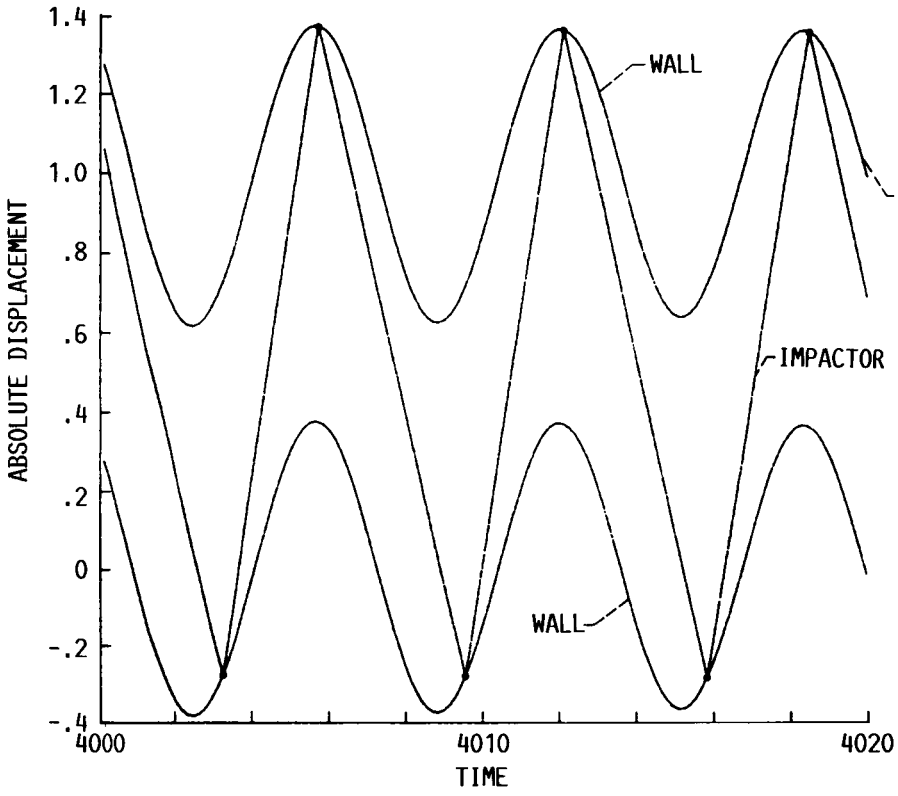

(A) AMPLITUDE, ~0.4; TWO UNEQUALLY SPACED IMPACTS PER CYCLE.

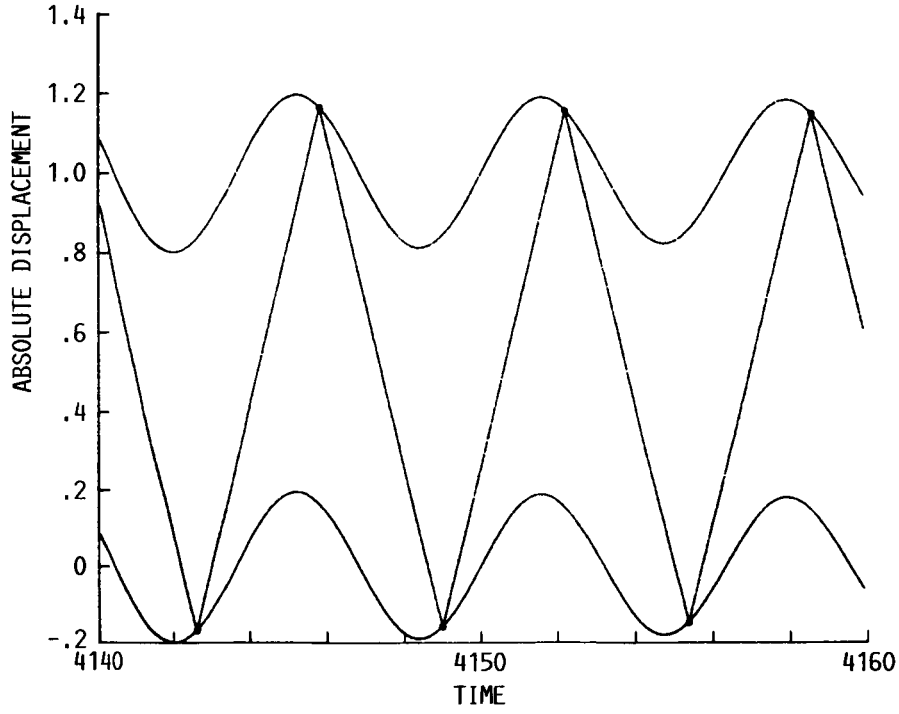

(B) AMPLITUDE, ~0.2; TWO EQUALLY SPACED IMPACTS PER CYCLE.

FIGURE 4. - IMPACT PATTERN. ABSOLUTE DISPLACEMENT OF IMPACTOR SHOWN TOGETHER WITH ABSOLUTE DISPLACEMENT OF CAVITY WALLS.

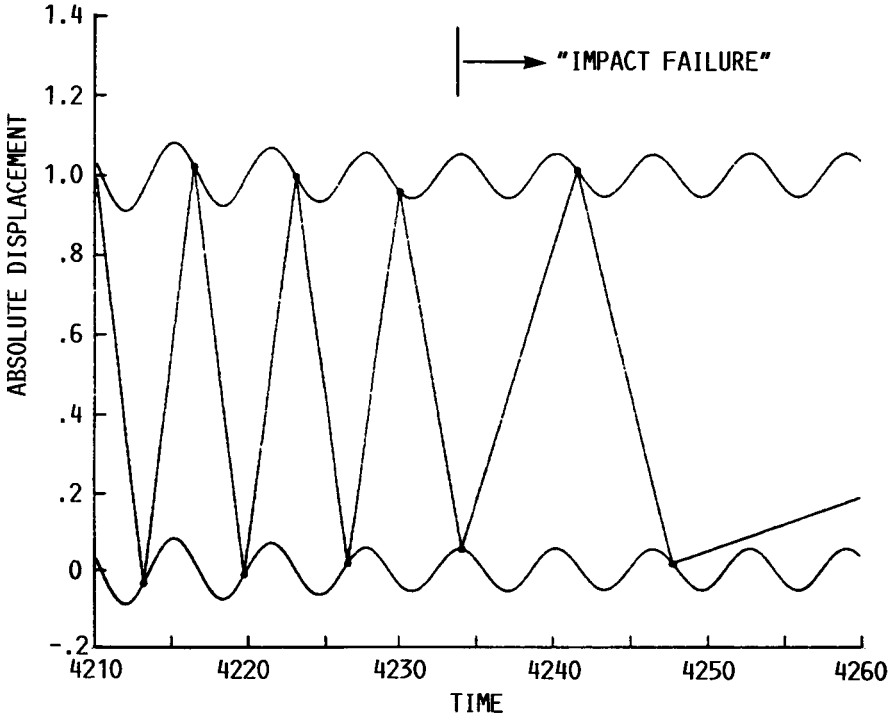

(C) AMPLITUDE, ~0.055; BEGINNING OF "IMPACT FAILURE."

FIGURE 4. - CONCLUDED.

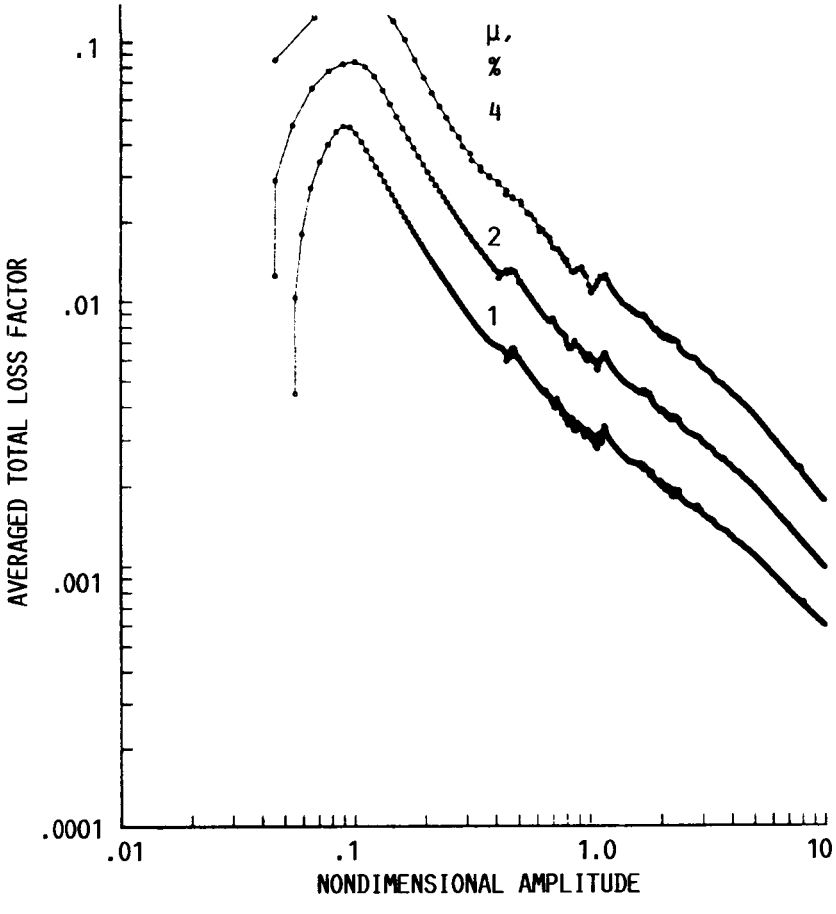

FIGURE 5. - AVERAGED TOTAL LOSS FACTOR AS A FUNCTION OF AMPLITUDE FOR THREE VALUES OF THE IMPACTOR MASS FRACTION. $\zeta = 0.0001$; $\varepsilon = 0.6$; $\mu = 1$ PERCENT; 2 PERCENT; AND 4 PERCENT.

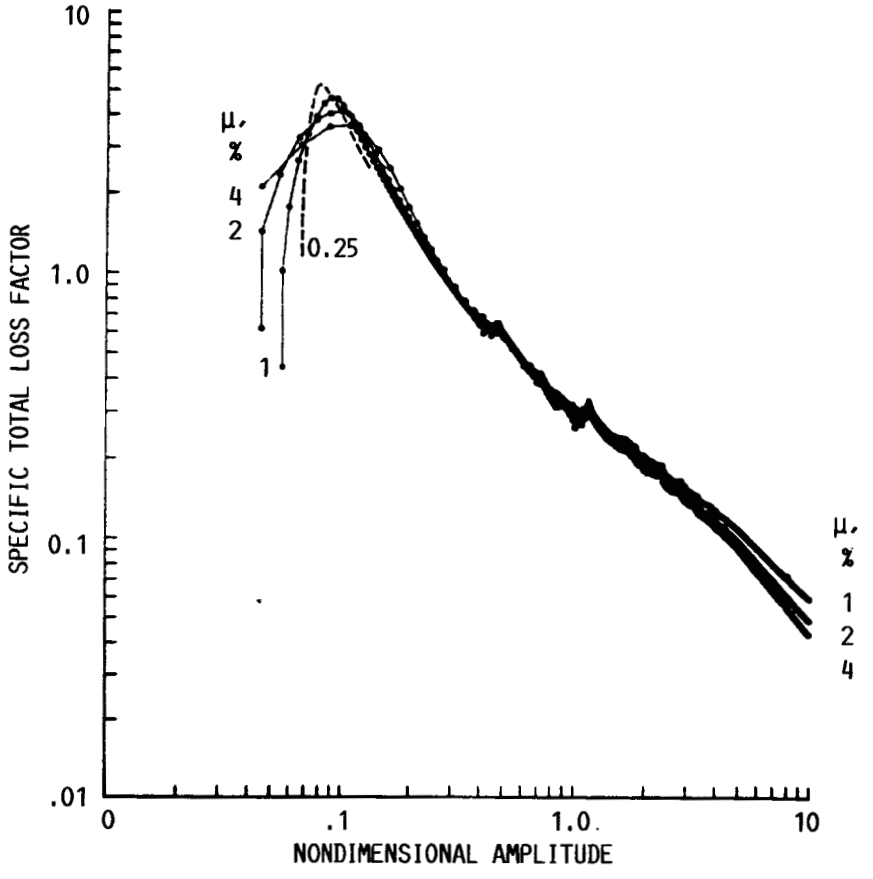

FIGURE 6. - SPECIFIC TOTAL LOSS FACTOR AS A FUNCTION OF AMPLITUDE. ζ = 0.0001; ε = 0.6; μ = 1 PERCENT; 2 PERCENT; AND 4 PERCENT.

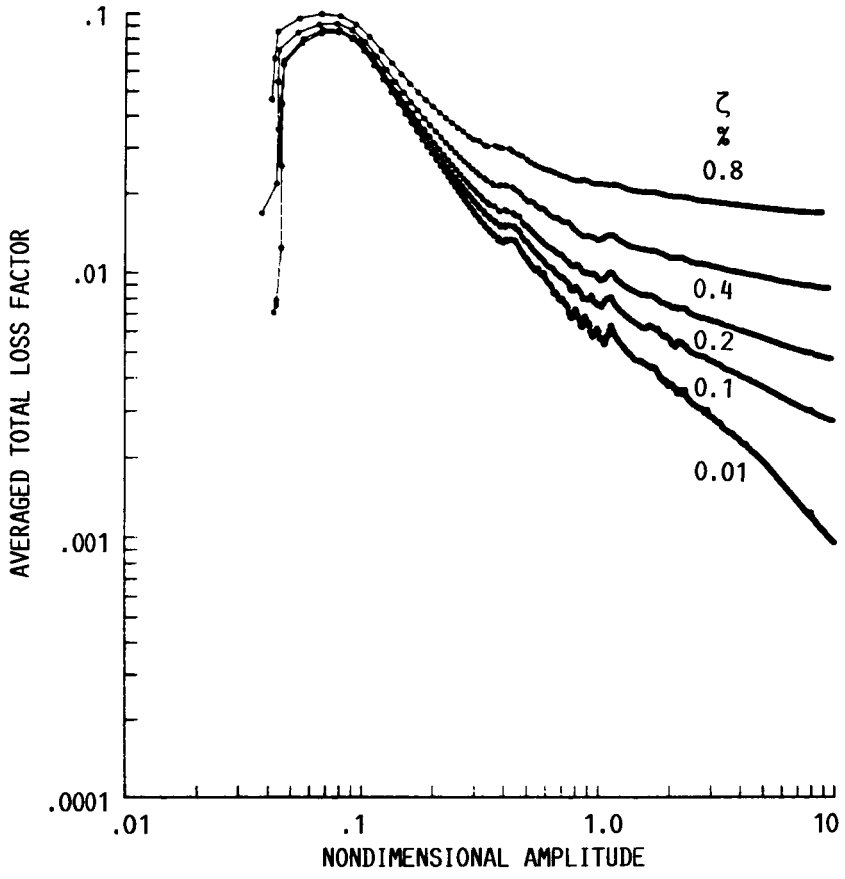

FIGURE 7. - TOTAL LOSS FACTOR FOR SEVERAL VALUES OF PROPORTIONAL DAMPING IN THE MAIN OSCILLATOR SYSTEM. μ = 2 PERCENT; ε = 0.6; ζ = .01 PERCENT; 0.1 PERCENT. 0.2 PERCENT; 0.4 PERCENT AND 0.8 PERCENT.

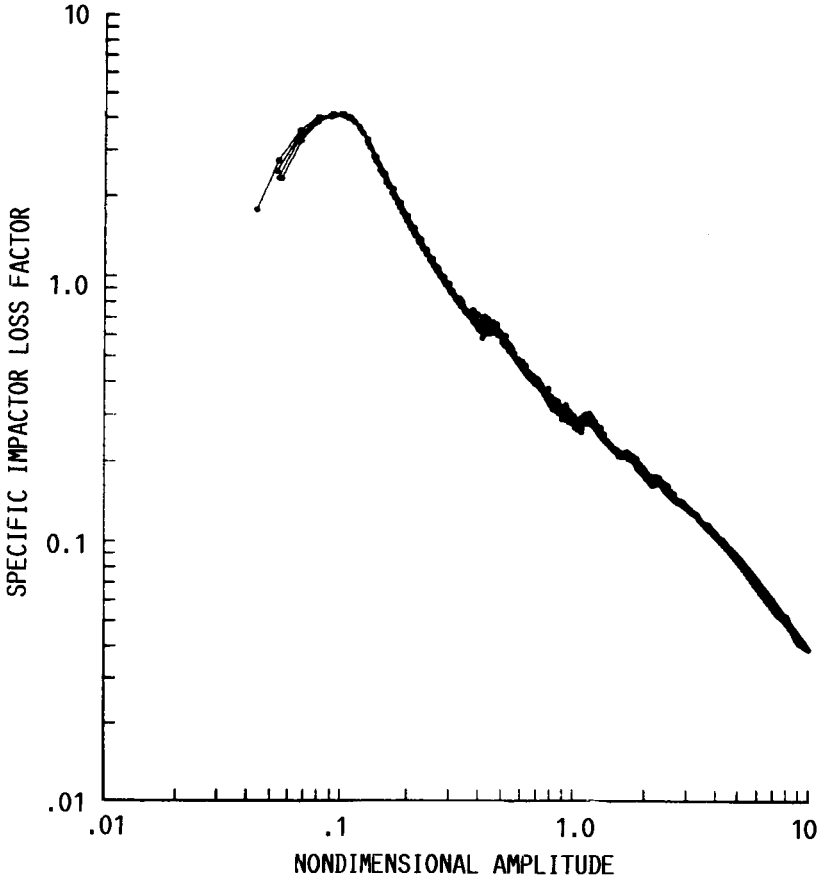

FIGURE 8. - SPECIFIC IMPACTOR LOSS FACTOR VERSUS AMPLITUDE. $\varepsilon = 0.6$. $\mu = 2$ PERCENT; $\zeta = 0.01$ PERCENT; 0.1 PERCENT; 0.2 PERCENT; 0.4 PERCENT; AND 0.8 PERCENT.

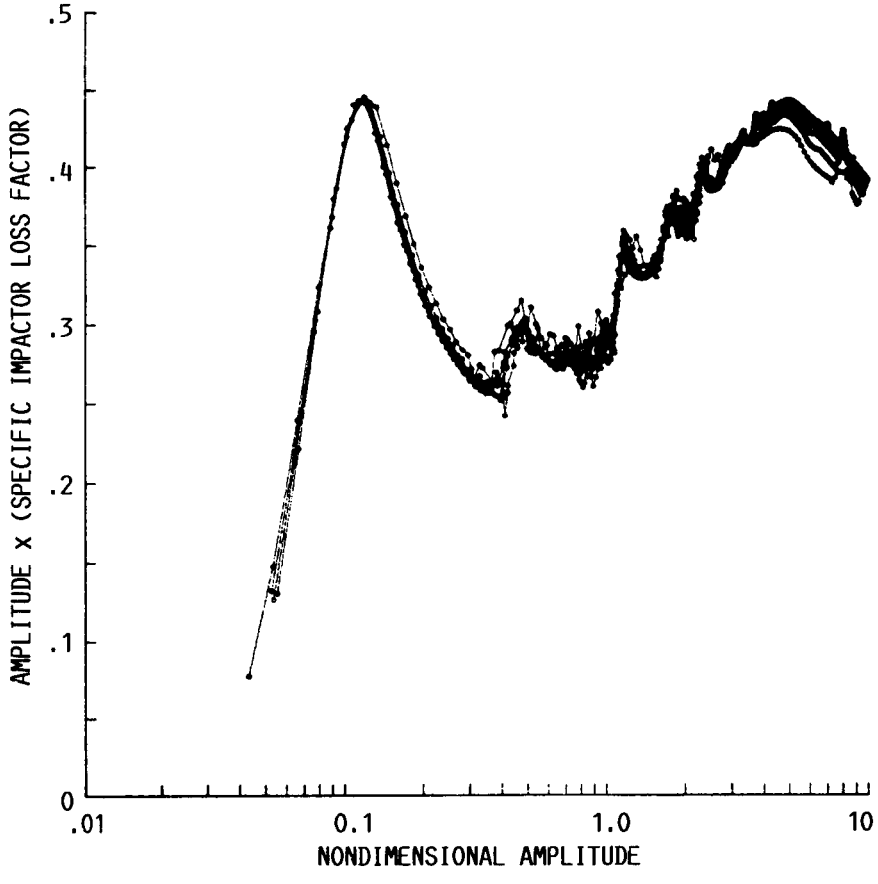

FIGURE 9. - AMPLITUDE TIMES SPECIFIC IMPACTOR LOSS FACTOR AS A FUNCTION OF AMPLITUDE. μ = 2 PERCENT; ζ = 0.01 PERCENT; 0.1 PERCENT; 0.2 PERCENT; 0.4 PERCENT; AND 0.8 PERCENT.

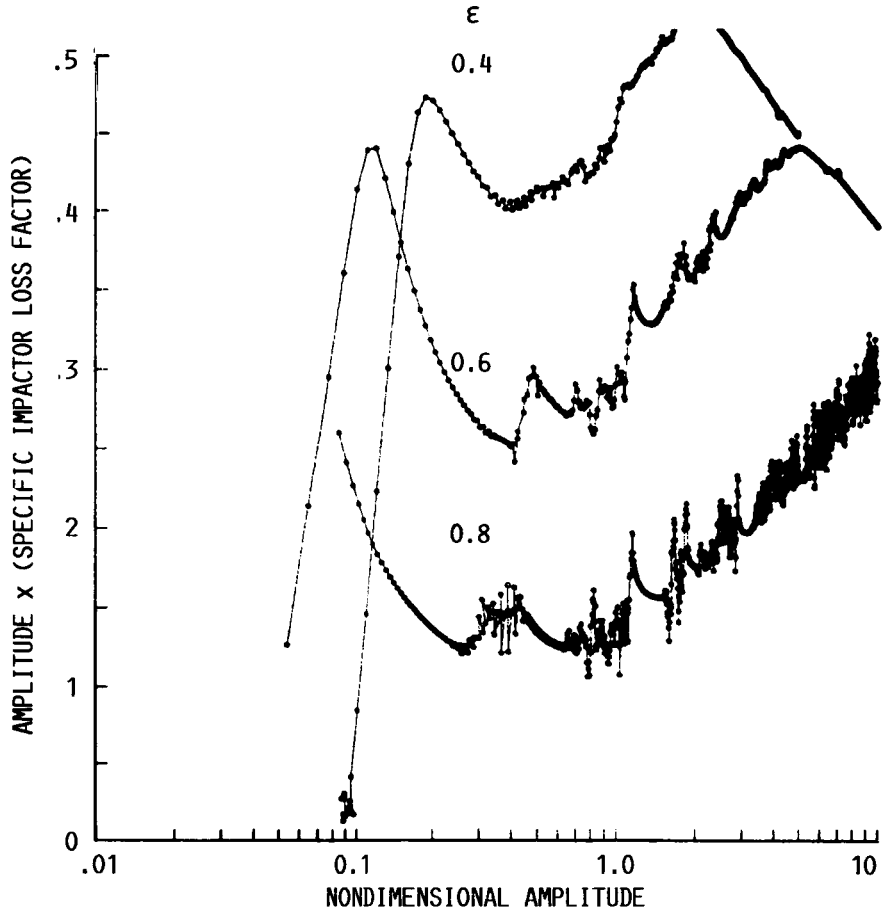

FIGURE 10. - AMPLITUDE TIMES SPECIFIC IMPACTOR LOSS FACTOR FOR THREE VALUES OF THE COEFFICIENT OF RESTITUTION. $\mu = 0.02$; $\zeta = 0.0001$; $\varepsilon = .4$; .6 AND .8.

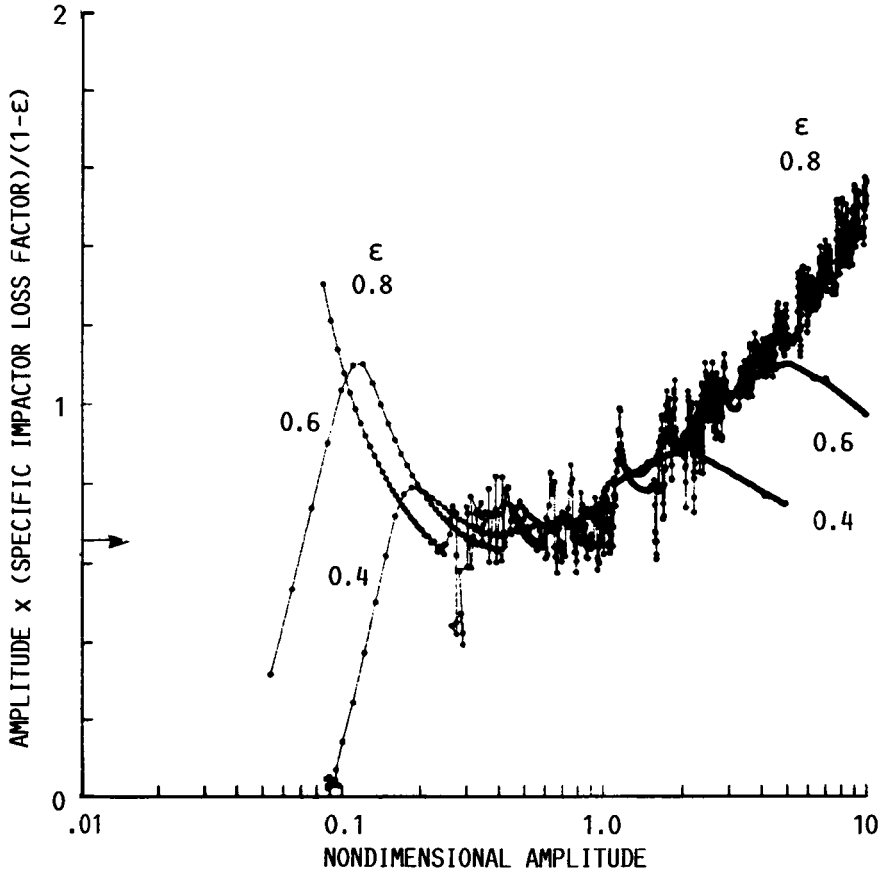

FIGURE 11. - AMPLITUDE TIMES SPECIFIC IMPACTOR LOSS FACTOR DIVIDED BY (1-ε) FOR THREE VALUES OF THE COEFFICIENT OF RESTITUTION. $\mu = 0.02$; $\zeta = 0.0001$; $\varepsilon = 0.4$; 0.6 AND 0.8.

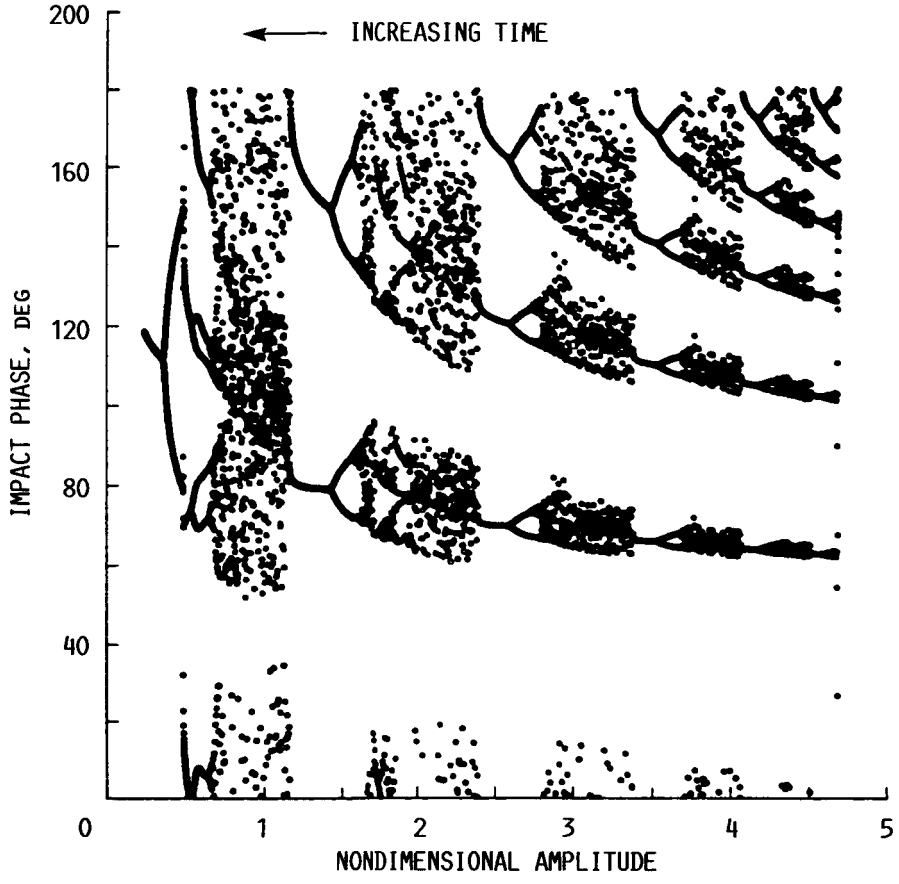

FIGURE 12. - IMPACT PHASE (MEASURED FROM OSCILLATOR ZERO CROSSING) AS A FUNCTION OF OSCILLATOR AMPLITUDE. $\mu = 0.00001$; $\zeta = 0.00025$; $\varepsilon = 0.6$.

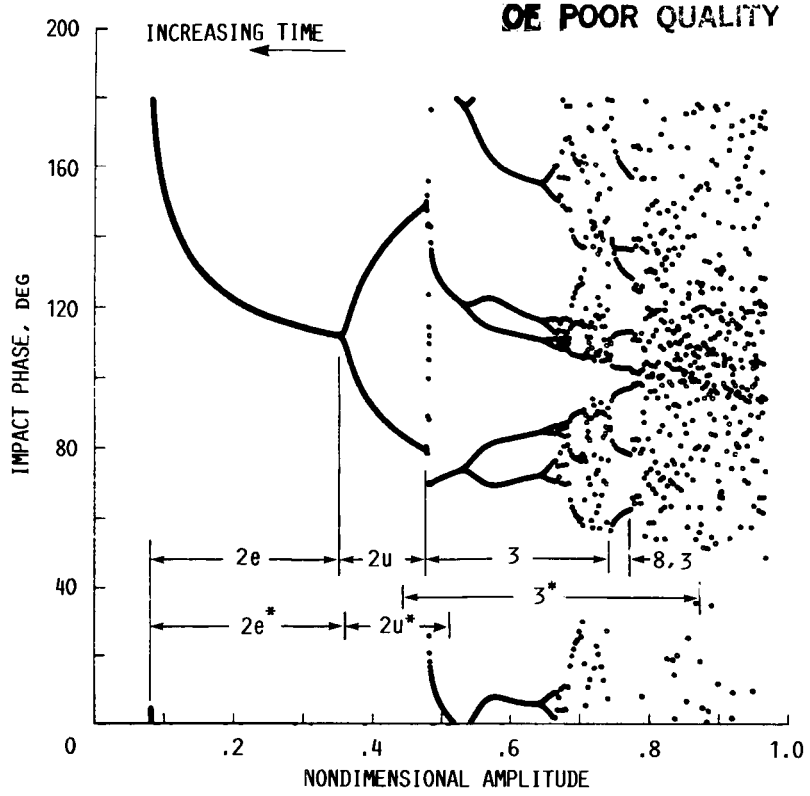

(A) DURING DECAY. $\zeta = 0.0002$

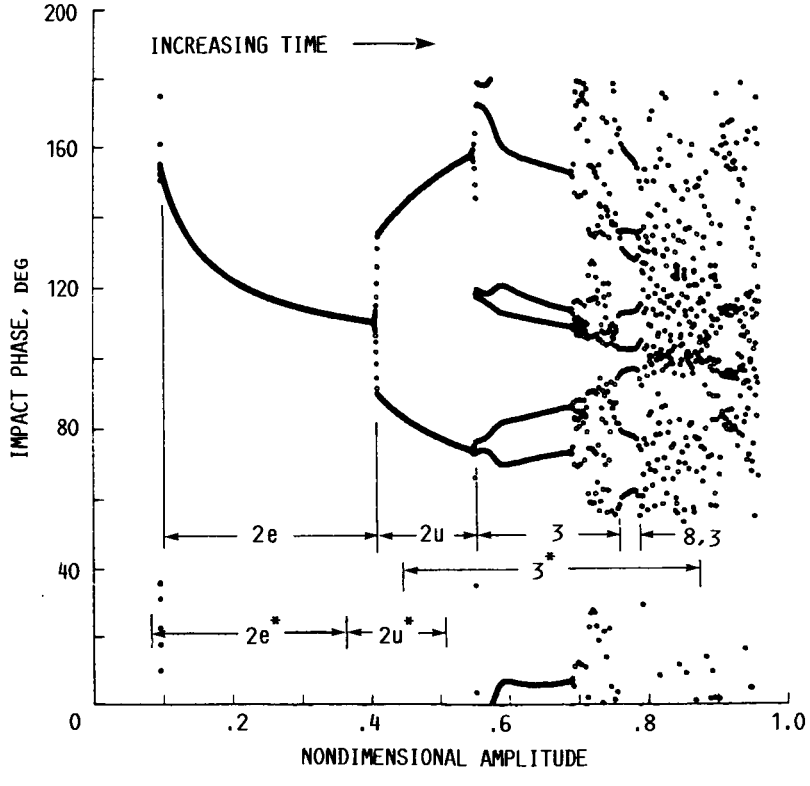

(B) DURING GROWTH. $\zeta = -0.0002$

FIGURE 13. - IMPACT PHASE AS FUNCTION OF AMPLITUDE.
$\mu = 0.00001$; $\varepsilon = 0.6$.

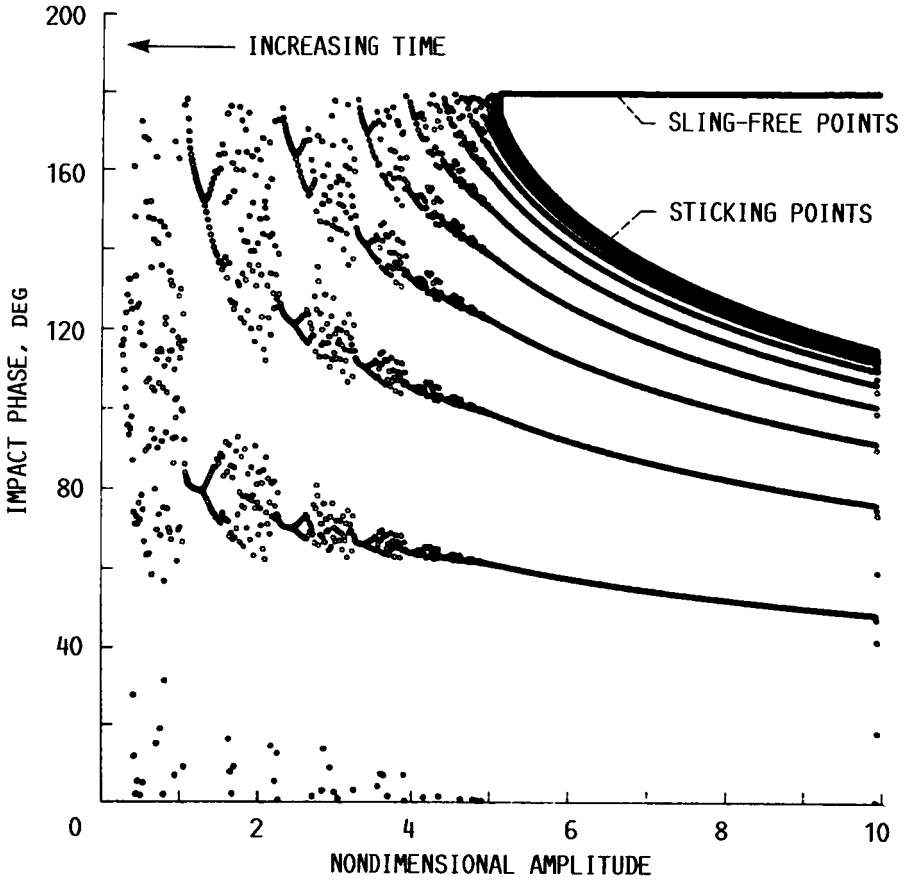

FIGURE 14. - IMPACT PHASE VERSUS OSCILLATOR AMPLITUDE FOR $\mu = 0.02$; $\zeta = 0.0001$; AND $\varepsilon = 0.6$.

1. Report No.	2. Government Accession No.	3. Recipient's Catalog No.
NASA TM-89897		

4. Title and Subtitle	5. Report Date
The Impact Damped Harmonic Oscillator in Free Decay	
	6. Performing Organization Code: 505-63-11

7. Author(s)	8. Performing Organization Report No.
G.V. Brown and C.M. North	E-3587
	10. Work Unit No.

9. Performing Organization Name and Address	11. Contract or Grant No.
National Aeronautics and Space Administration Lewis Research Center Cleveland, Ohio 44135	
	13. Type of Report and Period Covered: Technical Memorandum

12. Sponsoring Agency Name and Address	14. Sponsoring Agency Code
National Aeronautics and Space Administration Washington, D.C. 20546	

15. Supplementary Notes

Prepared for the Vibrations Conference sponsored by the American Society of Mechanical Engineers, Boston, Massachusetts, September 27-30, 1987. G.V. Brown, NASA Lewis Research Center; C.M. North, Rose-Hulman Institute of Technology, 5500 Wabash Avenue, Terre Haute, Indiana 47803.

16. Abstract

The impact-damped oscillator in free decay is studied by using time history solutions. A large range of oscillator amplitude is covered. The amount of damping is correlated with the behavior of the impacting mass. There are three behavior regimes: (1) a low amplitude range with less than one impact per cycle and very low damping, (2) a useful middle amplitude range with a finite number of impacts per cycle, and (3) a high amplitude range with an infinite number of impacts per cycle and progressively decreasing damping. For light damping the impact damping in the middle range is (1) proportional to impactor mass, (2) additive to proportional damping, (3) a unique function of vibration amplitude, (4) proportional to $1-\varepsilon$, where ε is the coefficient of restitution, and (5) very roughly inversely proportional to amplitude. The system exhibits jump phenomena and period doublings. An impactor with 2 percent of the oscillator's mass can produce a loss factor near 0.1.

17. Key Words (Suggested by Author(s))	18. Distribution Statement
Damping; Impact damping; Harmonic oscillator; Chaos; Impact damper	Unclassified - unlimited STAR Category 37

19. Security Classif. (of this report)	20. Security Classif. (of this page)	21. No. of pages	22. Price*
Unclassified	Unclassified	22	A02

*For sale by the National Technical Information Service, Springfield, Virginia 22161